

Side-Wall Functionalization of Single-Walled Carbon Nanotubes with 4-Hydroxymethylaniline Followed by Polymerization of ϵ -Caprolactone

Fabian Buffa,[§] Hui Hu,[‡] and Daniel E. Resasco^{*,†}

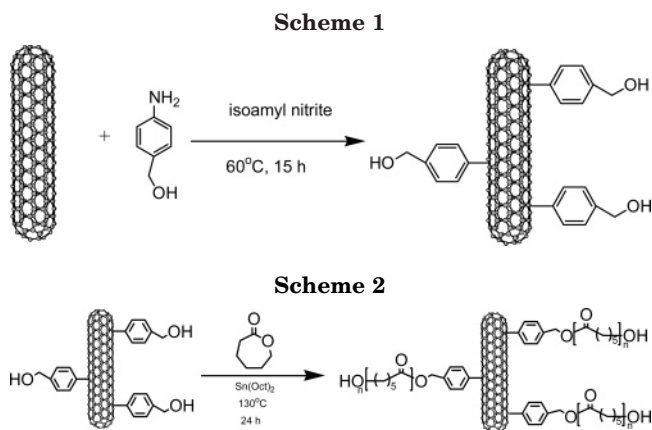
School of Chemical, Biological, and Materials Engineering, University of Oklahoma, Norman, Oklahoma 73019; SouthWest Nanotechnologies, Inc. (SWeNT), Norman, Oklahoma 73069; and F. Ingenieria, INTEMA, Universidad Nac. Mar del Plata, Argentina

Received April 24, 2005; Revised Manuscript Received July 27, 2005

ABSTRACT: Nanotube functionalization with 4-hydroxymethylaniline (HMA) via the diazonium salt method has been done on SWNT produced by the CoMoCAT process. Thermal analysis indicates 1 out of every 33 C atoms remains functionalized. Raman, FTIR, and optical absorption spectroscopy confirm the side-wall functionalization and show that it can be reversed by thermolysis. The OH group that is generated from the functionalization was used to start the ring-opening polymerization of ϵ -caprolactone. The polymer thus produced (PCL) remains grafted to the nanotube as demonstrated by FTIR and a dramatic increase in suspendibility in chloroform. By combining several techniques (TGA, TPD, and TPO) a quantification of the number of polymer chains attached to the nanotube and their average length has been attempted.

1. Introduction

Because of their exceptional electronic and mechanical properties, single-walled carbon nanotubes (SWNTs) have stirred the interest of academic and industrial researchers worldwide.^{1,2} However, several technical challenges need to be overcome before the extraordinary properties of these unique materials can be fully utilized. For example, as produced SWNT are typically bound into intertwined bundles that exhibit very low solubility in either water or organic solvents. Several approaches have been investigated to improve dispersion and solubility of nanotubes, such as milling,^{3,4} ultrasonication,⁵ and high-shear-flow mixing,⁶ combined with the addition of surfactants and dispersing agents.^{7,8} Another approach that has opened a large number of research opportunities and potential applications is chemical functionalization. Some of the functionalization approaches previously reported have involved the formation of covalent bonds^{9–12} while others have employed noncovalent interactions.^{13–16} The initial attempts for covalent functionalization took advantage of the higher reactivity of carbon atoms at the ends of the nanotubes to carry out the series of reaction steps leading to the covalent attachment. The disadvantage of this type of functionalization is that only a small fraction of the carbon in the nanotube becomes functionalized.¹⁷ More recent approaches have made side-wall functionalization possible with high functionality-to-carbon ratio.^{10–12} This type of side-wall covalent functionalization significantly alters the optical properties of the nanotubes due to the modifications introduced in the graphene structure. As a result, spectroscopic techniques such as UV–vis–NIR optical absorption and Raman can be effectively used to monitor the extent of functionalization. In addition, side-wall functionalization provides anchoring sites at the nanotube wall to



improve the interaction of the nanotube with a polymeric matrix.

In this contribution, we report a novel functionalization that follows the approach of the diazonium salts developed by Tour et al.,^{11,12,18} but in this case, we have employed 4-hydroxymethylaniline (HMA) as the reagent for the generation of the diazonium salt (see Scheme 1). The purpose of using HMA is to leave the functionalized nanotube with a nonphenolic OH group accessible for further reaction in order to start the ring-opening polymerization (ROP) of ϵ -caprolactone. We show here that, by this route, an effective anchoring of the resulting polymer to the nanotubes can be attained. As illustrated in Scheme 2, the grafted polymer that results should have a structure similar to that of star polymers of PCL^{19–22} and represents a novel example of the nanotube–polymer composite of the type known as “grafted-from”.^{23–26} We have chosen polycaprolactone due to its potential applications in the biomedical industry.^{27,28} While it has good water, oil, solvent, and chlorine resistance, polycaprolactone is fully biodegradable, biocompatible, and nontoxic to living organisms. It has been used in the development of controlled drug delivery systems as well as in surgical sutures and other resorbable fixation devices. The potential uses of this polymer in tissue engineering have prompted us to

[†] University of Oklahoma.

[‡] SouthWest Nanotechnologies, Inc.

[§] Universidad Nac. Mar del Plata.

* To whom correspondence should be addressed: e-mail resasco@ou.edu.

investigate the grafting to the side walls of single-walled carbon nanotubes.

2. Experimental Section

The nanotubes used in this study have been obtained by the catalytic CoMoCAT method developed in our group,²⁹ which employs a silica-supported Co–Mo powder to catalyze the selective growth of single-walled carbon nanotubes by disproportionation of CO. As previously shown, adjustment of the reaction parameters allows for a fine control of the nanotube structure.^{30,31} The nanotubes used in this study have an average diameter of 0.8 nm and have majority of (6,5) among the semiconducting nanotubes present in the sample.³² The SWNT grown by this method remain mixed with the spent catalyst, containing the silica support and the catalytic Co and Mo species, which are eliminated in a two-step purification step. First, the raw material is placed in an oven at 250 °C for 10 h to oxidize the Co and Mo species remaining in the product. The second step is the dissolution of the catalyst in HF solution (33% in water), followed by thorough washing in water. The resulting nanotube material has an excellent quality, as verified by TEM, SEM, and the D/G band ratio in the Raman spectra obtained at laser excitations of 633, 514, and 488 nm, as well as a low impurity content (less than around 10 wt % of Co, Mo, and Si oxides and carbides), as determined by XPS analysis.

The functionalization was carried out following a methodology similar to that established by Tour et al.¹⁸ In a typical experiment, a 20 mg (1.67 mmol) sample of SWNT was horn-sonicated for 30 min in 25 mL of *o*-dichlorobenzene, using a Fisher Scientific model 550 homogenizer (550 W output) operated at 35% amplitude. This suspension was placed in a two-neck round-bottom glass flask together with a solution of 0.788 g (6.4 mmol) HMA in 12.3 mL of acetonitrile. With a reflux condenser in one of the flask necks, the mixture was stirred for 10 min by bubbling nitrogen. Next, 1.17 g (10 mmol) of isoamyl nitrite was added to the mixture, which was then heated to 60 °C and kept at this temperature for 15 h, under continuous stirring. After cooling to 35–45 °C, the mixture was diluted with 75 mL of dimethylformamide (DMF) and filtered through a PTFE membrane (0.2 μm pore size). The solid retentate was first washed with copious amounts of DMF and then further washed in sequential cycles of sonication in 2-propanol (30 min each), followed by filtration until the liquid filtrate came out colorless. The resulting purified solid was vacuum-dried overnight at room temperature.

To quantify the degree of functionalization, a combined TPD/TPO technique was employed. This is an in-house built unit consisting of a flow reactor cell connected to a gas chromatograph (HP 5890). The reactor cell, in which a known amount of solid sample is placed, is heated with a linear ramp in an oven controlled by a programmable temperature controller. In the TPD mode (TPD = temperature-programmed desorption), the functionalized nanotubes were heated in a linear temperature ramp up to 650 °C in flowing He. The exit stream was directly connected to a flame ionization detector (FID), whose signal was calibrated to quantitatively determine the moles of carbon atoms. In the TPD stage, thermolysis causes the evolution of the functional groups, which are oxidized and quantitatively detected in the FID. In the TPO mode (TPO = temperature-programmed oxidation), the regenerated pristine nanotubes are oxidized and converted to CO and CO₂, which are subsequently quantitatively converted to CH₄, which is detected and measured in the FID. The combined TPD/TPO measurements indicated that 1 out of every 33 carbon atoms was functionalized. We estimate that the error in this measurement is less than 10%.

Detailed characterization of the nanotubes after the various steps investigated was carried out by a combination of Raman spectroscopy, optical absorption, TEM, and SEM. The Raman spectra were obtained in a Jovin Yvon-Horiba LabRAM HR-800 equipped with a CCD detector and with three different laser excitation sources, having wavelengths of 633 nm (He–Ne laser) and 514 and 488 nm (Ar laser). This system is

equipped with an in-situ reaction chamber that can be heated to more than 1000 °C under flowing gases. To study the thermolysis of the functionalized nanotubes, the sample was placed in the in-situ cell and then exposed to a continuous flow of pure He while the temperature was increased up to 400 °C and kept at that temperature for either 30 or 60 min. After heating was stopped, Raman spectra were obtained at room temperature under the same flow. Functionalized and defunctionalized samples were analyzed by optical absorption in DMF suspensions. The suspensions were prepared by horn-sonicating the SWNT samples in DMF (~0.01 mg/mL) for 15–30 min. Also, pristine SWNT were analyzed in surfactant suspension by adding them to an aqueous solution containing sodium dodecylbenzenesulfonate (SDBS) at twice its critical micelle concentration and horn-sonicated for 1 h. This procedure generated a stable suspension of individual and bundled nanotubes, which was then centrifuged for 1 h at 15 000 rpm to separate residual metallic catalyst particles and suspended bundles from the lower density surfactant-suspended individual nanotubes. Finally, the supernatant liquid was withdrawn for spectral analysis. The absorption of light as a function of wavelength was measured using a Bruker Equinox 55 FTIR/FTNIR/FTVis; 60 scans at 30 cm⁻¹ resolution were averaged on each spectrum in order to achieve a high signal-to-noise ratio.

The SEM images of the solid samples were obtained in a JEOL 880 scanning microscope. Solid samples of the pristine, functionalized, and polymer-attached SWNT were also studied by FTIR in the Bruker Equinox 55 to investigate the presence of different functional groups. In these measurements, pellets of solid samples were prepared mixing the nanotubes with KBr.

The nanotube-based polymerization of ϵ -caprolactone was carried out via the ring-opening reaction (ROP) in which the OH groups present in the nanotube-grafted functionalities acted as initiators of the polymerization reaction. The ROP is catalyzed by tin 2-ethylhexanoate, and it is well-known that it follows an insertion–coordination mechanism. In the particular experiment conducted in this case, 10 mg (0.83 mmol) of functionalized SWNT was suspended in 15 mL of *o*-dichlorobenzene by sonicating with the horn sonicator (35% amplitude) for 30 min. The suspension was then transferred to a two-neck vessel (absolutely dry) and mixed with 2 mL (18.66 mmol) of ϵ -caprolactone (Aldrich, 99%) and Sn(Oct)₂ catalyst (Aldrich, 95%) (0.1% molar with respect to ϵ -CL) under nitrogen flow. The two-neck vessel was then connected to a reflux condenser where the ROP reaction was allowed to occur in the liquid phase, under nitrogen constantly bubbling, for 24 h at 130 °C. At the end of this reaction period, the hot liquid was transferred from the vessel into a beaker containing cold *n*-hexane, which caused the precipitation of the polymeric material, which was subsequently filtered through a PTFE membrane and copiously washed with the solvent. Afterward, to eliminate the free polymer, the solid retentate was treated with 30 mL of chloroform at room temperature, since free PCL is very soluble in chloroform. The remaining black solid was washed several times with more chloroform. To confirm the absence of any free polymer, a few drops of filtrate were contacted with *n*-hexane. The absence of any precipitate confirmed that no free polymer remained after the thorough washing process. The final solid was dried overnight in a vacuum at room temperature. The resulting SWNT/PCL composite was characterized by TGA and DSC. The TGA were conducted in a Shimadzu TGA-50, under air at a heating rate of 5 °C/min, from room temperature to 800 °C. The DSC was conducted in a Perkin-Elmer, model Pyris 1 at a heating rate of 10 °C/min from –30 to 150 °C under a flow of nitrogen.

3. Results and Discussion

The formation of covalent bonds following the functionalization procedure was confirmed by FTIR. The mid-IR spectrum of the purified nanotubes is shown in Figure 1a. The most distinct features are two bands that can be ascribed to the stretching modes of OH groups

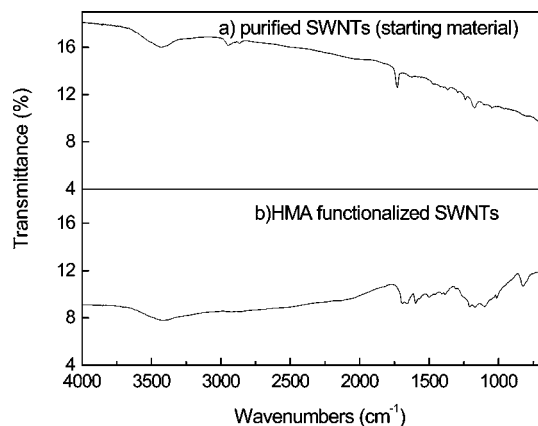


Figure 1. FTIR spectra of (a) purified SWNT (starting material) and (b) HMA-functionalized SWNTs.

(3430 cm^{-1}) and C=O groups (1726 cm^{-1}). Similar bands have been previously observed on acid-purified SWNT and typically ascribed to carboxylic acid groups located at defects and/or ends of nanotubes. A significant change is observed in the spectrum obtained after the functionalization routine shown in Figure 1b. New bands provide evidence for the presence of functional groups definitely bound to the nanotubes. The presence of the aromatic ring (stretching C–C, 1598 cm^{-1} , bending C–H, 827 cm^{-1}), the CH₂ group (1384 cm^{-1}), and the alcoholic C–OH (bending, 1500 cm^{-1} ; stretching, 1103 cm^{-1}) is positively demonstrated.

Figure 2 illustrates the Raman spectra of the nanotubes after the different steps using an excitation laser with wavelength 633 nm . Comparing parts a and b of Figure 2, a drastic difference in the relative intensity of the D band (1290 cm^{-1}) with respect to the main G band is evident. The increase in the D band has been previously reported³³ and used as an indication of covalent side-wall functionalization, as it reflects the conversion of the hybridization of some C atoms on the nanotube wall from sp^2 to sp^3 . At the same time, the heavy functionalized nanotubes show the disappearance of the RBM bands in the low-frequency region. Finally, as shown in Figure 2c, when the functionalized material was heated to $400\text{ }^\circ\text{C}$ in pure He for 30 min, the original Raman spectrum was almost restored. That is, the D/G band ratio became again very low and the RBM bands reappeared, which, as previously shown,³³ indicate the recovery of the delocalized π system in the SWNTs and demonstrate that the removal of the functionalities by thermolysis leaves the CoMoCAT nanotubes intact. In fact, a closer examination reveals that a small difference in the size and shape of the D bands of the pristine and regenerated nanotubes exists. Also, the suspendibility of the nanotubes is clearly different. This effect is illustrated in Figure 3, which compares the UV–vis–NIR absorption spectra of the three samples suspended in DMF after horn sonication for 15–30 min with the pristine SWNT suspended in SDDBS surfactant solution. On the material suspended in the surfactant solution (Figure 3) prominent bands near 976 and 566 nm are clearly observed, and they correspond to the S11 and S22 transitions of the (6,5) nanotube,³⁴ which constitutes the majority of the semiconducting nanotubes present in the CoMoCAT material.³² DMF was not so effective as the surfactant to exfoliate the bundles. As a result, even for the pristine nanotube samples, the absorption bands are much less intense and broader than those obtained with SDDBS.

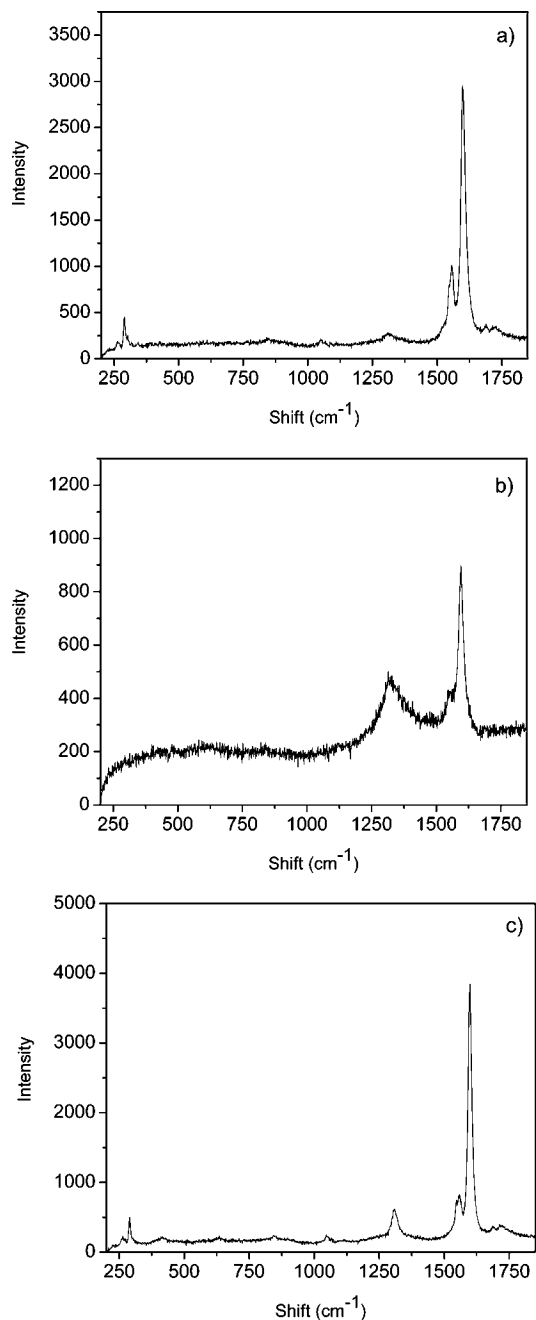


Figure 2. Raman spectra (633 nm excitation) of (a) SWNT, (b) HMA-functionalized nanotubes, and (c) defunctionalized nanotubes after heating in He at $400\text{ }^\circ\text{C}$.

After functionalization the bands completely disappear due to the disruption of the π system by the newly formed covalent bonds. This disappearance has been previously seen and interpreted in this way.³³ However, to our knowledge, the optical absorption spectrum of the regenerated nanotubes after thermolysis of the functionalities has not been reported before. It is important to note that, despite a strong recovery of the Raman spectrum, the reversibility of the optical absorption is only partial. In fact, absorption bands are indeed observed to come back, which confirms the elimination of the functionalities and the restoration of the π system, but the bands are now broader and of lower intensity than those of the pristine nanotubes. This difference might indicate that the defunctionalized, regenerated, nanotubes have a lower dispersibility in DMF than the original nanotubes.

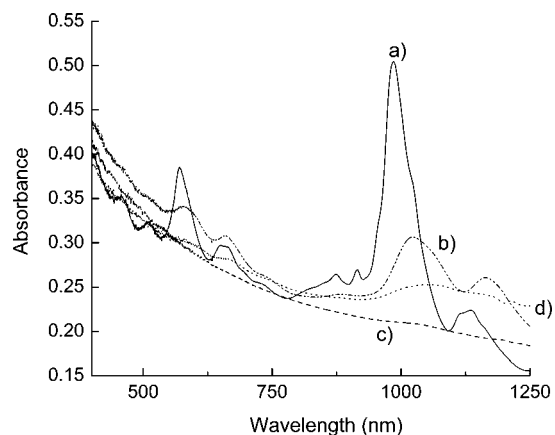


Figure 3. Absorption spectra of (a) pristine SWNT suspended in SDDBS surfactant solution, (b) pristine SWNT suspended in DMF, (c) HMA-functionalized nanotubes suspended in DMF, and (d) defunctionalized nanotubes after heating the HMA-functionalized sample at 400 °C, suspended in DMF.

Another interesting comparison of the microstructure of the material after the different procedures was made by SEM. The state of aggregation of the pristine, functionalized, and regenerated nanotubes is illustrated in parts a, b, and c of Figure 4, respectively. It is interesting to point out the “ribbonlike” structure of the 12–25 nm bundles observed for the functionalized nanotubes. It is possible that the presence of –OH groups on the functionalized nanotubes generate hydrogen-bond-type interactions. By contrast, the regenerated sample shows a bundle morphology that looks very similar to that of the pristine nanotubes. However, although the morphology as observed by SEM shows no significant differences, both Raman and the lower suspendability of the sample after defunctionalization indicates that the reversibility is not complete.

The characterization of the nanotube-grafted PCL material was conducted by FTIR spectroscopy. As shown in Figure 5, when the mid-IR spectrum is compared to that of the corresponding functionalized material without polymer, new bands are clearly seen. One of them appears at 2924 cm^{-1} and is ascribed to the stretching mode of the CH_2 groups of the PCL. Another band that becomes more prominent is the one at 1726 cm^{-1} , which can be assigned to the carbonyl group of the ester group present in the polymer. Although this band was present in the pristine nanotubes resulting from carboxylic acid groups, now it is much more intense. The presence of the ester groups is also demonstrated by the bands at 1157 and 1095 cm^{-1} , which correspond to the stretching of the C–O single bond of the ester bonds in the polymer.

In addition, the suspendability of the nanotube-grafted PCL in chloroform was compared to that of a comparable amount of functionalized nanotubes. As mentioned above, PCL is very soluble in chloroform, and we expect that an effective anchoring of the polymer to the nanotubes could impart a higher suspendability to the nanotubes. To conduct this comparison, 2 mg of functionalized nanotubes (SWNT-HMA) and nanotube-grafted PCL (SWNT-HMA-PCL) were placed in separate vials. 10 mL of chloroform was added to each vial followed by horn sonication for 20 min (35% amplitude). A remarkable difference in suspendability was observed. As illustrated in Figure 6, while the SWNT-HMA sample could not be suspended in chloroform, a stable

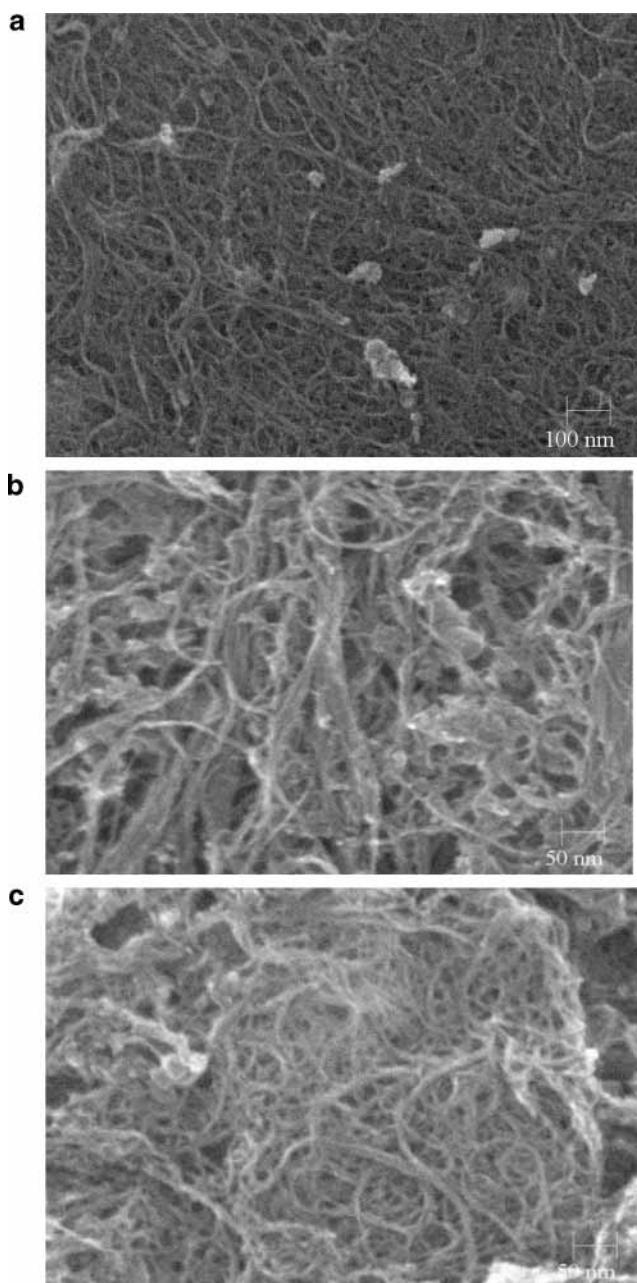


Figure 4. SEM images of (a) pristine SWNT, (b) HMA-functionalized nanotubes, and (c) defunctionalized nanotubes after heating the HMA-functionalized sample at 400 °C.

suspension was generated with the SWNT-HMA-PCL sample.

The TGA thermograms were used to determine the relative amount of polymer grafted onto the nanotubes. As shown in Figure 7, the attached polymeric chain starts decomposing at $\sim 200\text{ °C}$, together with the functional groups, while the SWNT remain stable up to about 450 °C , at which temperature they start oxidizing. With such a wide difference in stability it is possible to measure the amounts of polymer and SWNT in a given sample. Accordingly, these results indicate that about 37 wt % of the sample is composed by SWNT while the remaining 63 wt % can be ascribed to the combination of polymer and functionalities. Therefore, taking into account that the combined TPD/TPO measurements indicated 1 functionality every 33 C atoms (± 3) in the SWNT, and assuming that a polymer chain grows from each functionality, one can calculate the

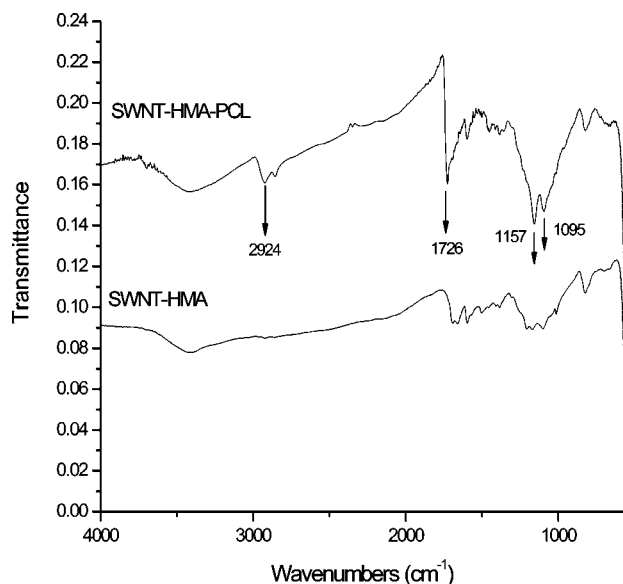


Figure 5. FTIR spectra of (a, top) nanotube-grafted polycaprolactone (SWNT-HMA-PCL) after functionalization with HMA and ring-opening polymerization of caprolactone and (b, bottom) HMA-functionalized SWNT (same as Figure 1b).

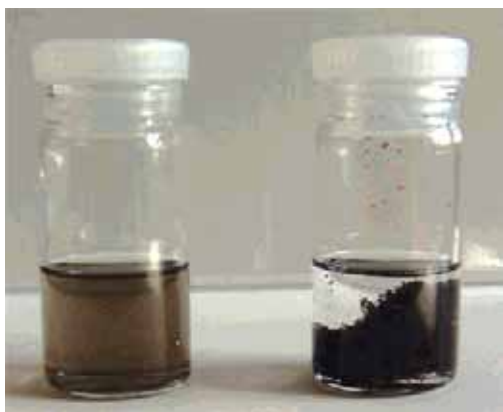


Figure 6. Comparison of chloroform suspensions of (a, left) nanotube-grafted polycaprolactone (SWNT-HMA-PCL) after functionalization with HMA and ring-opening polymerization of caprolactone and (b, right) HMA-functionalized SWNT.

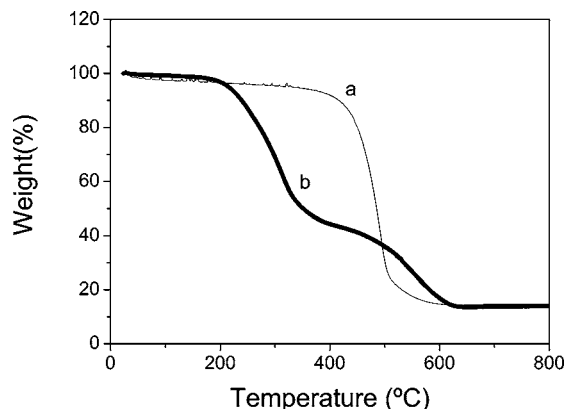


Figure 7. Thermal gravimetry analysis (TGA in air) of the SWNT (a) and SWNT/PCL composite (b).

average length of the PCL chain. Accordingly, short chains of five CL units in average can be estimated. This is indeed a very short chain length. Two reasons can be proposed to explain this short length. In the first place, the presence of nanotubes in the polymerization me-

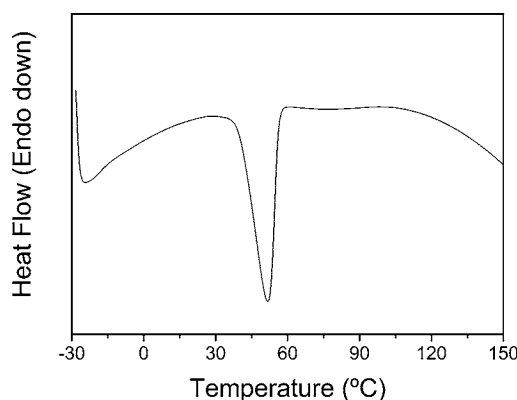


Figure 8. Differential scanning calorimetry (DSC in nitrogen) thermogram of the SWNT-PCL sample.

dium may act as terminators of the chain growth, which will limit the chain length. At the same time, we believe that it is possible that there is water adsorbed on the nanotube surface, and each adsorbed water molecule can act as an initiator of the ring-opening polymerization, generating as a result a large amount of free PCL. Accordingly, to increase the length of the PCL attached to the nanotubes, one should eliminate the adsorbed water from the nanotubes.

Further information about the nature of the polymer chains can be obtained from the DSC thermogram shown in Figure 8. The single endothermic peak appearing at 52 °C is due to the melting of the polymer; the integration of the area of this peak relative to the amount of polymer in the composite yields the specific heat of fusion. The resulting value of 29 J/g is low and would correspond to a 20% crystallinity of the polymer, based on a heat of fusion of 16.9 kJ/mol of repeating units when crystallinity is 100%.³⁵ This low degree of crystallinity is consistent with the short chains predicted above and with the possible structural disorder imparted by the presence of the SWNT.

4. Conclusions

Functionalization with 4-hydroxymethylaniline (HMA) has allowed us to achieve a successful grafting of poly- ϵ -caprolactone (PCL) to SWNT prepared by the Co-MoCAT process, which contain the majority of (6,5) semiconducting nanotubes. The PCL-modified nanotubes show a markedly increased suspendibility in chloroform due to the high solubility of PCL in this solvent. The impact of PCL as a biodegradable and biocompatible polymer, and its applications in tissue engineering give significance to these results, which could lead to the incorporation of nanotube-based advanced materials for biomedical purposes. At the same time, these results can be generalized to other monomers that polymerize via the same mechanism as PCL as well as to the generation of copolymers by using appropriate combinations of monomers. Also, the terminal OH groups of the grafted PCL can be used for further functionalization or attachment to other matrices.

Acknowledgment. This research was conducted with financial support from the Department of Energy, Office of Basic Energy Sciences (DE-FG03-02ER15345), and the National Science Foundation (CTS-0308619).

References and Notes

- (1) Iijima, S. *Nature (London)* **2001**, *13*, 3823–3824.
- (2) Dresselhaus, M. S.; Dresselhaus, G.; Avouris, P., Eds.; *Carbon Nanotubes: Synthesis, Structure, Properties and Applications*; Springer-Verlag: Heidelberg, Germany, 2001.
- (3) Li, Y. B.; Wei, B. Q.; Liang, J.; Yu, Q.; Wu, D. H. *Carbon* **1999**, *37*, 493–497.
- (4) Kim, Y. A.; Hayashi, T.; Fukai, Y.; Endo, M.; Yanahisawa, T.; Dresselhaus, M. S. *Chem. Phys. Lett.* **2002**, *355*, 279–284.
- (5) Shelimov, K. B.; Esenaliev, R. O.; Rinzler, A. G.; Huffman, C. B.; Smalley, R. E. *Chem. Phys. Lett.* **1998**, *282*, 429–434.
- (6) Hilding, J.; Grulke, E. A.; Zhang, Z. G.; Lockwood, F. J. *Dispersion Sci. Technol.* **2003**, *24*, 1–41.
- (7) Riggs, J. E.; Walker, D. B.; Carroll, D. L.; Sun, Y. P. *J. Phys. Chem. B* **2000**, *104*, 7071–7076.
- (8) Matarredona, O.; Rhoads, H.; Li, Z.; Harwell, J.; Balzano, L.; Resasco, D. *J. Phys. Chem. B* **2003**, *107*, 13357–13367.
- (9) Bahr, J. L.; Yang, J.; Kosynkin, D. M.; Bronikowski, M. J.; Smalley, R. E.; Tour, J. M. *J. Am. Chem. Soc.* **2001**, *123*, 6536–6542.
- (10) Pompeo, F.; Resasco, D. *Nano Lett.* **2002**, *2*, 369–373.
- (11) Dyke, C. A.; Tour, J. M. *Nano Lett.* **2003**, *3*, 1215–1218.
- (12) Strano, M. S.; Dyke, C. A.; Usrey, M. L.; Barone, P. W.; Allen, M. J.; Shan, H.; Kittrell, C.; Hauge, R. H.; Tour, J. M.; Smalley, R. E. *Science* **2003**, *301*, 1519–1522.
- (13) Chen, J.; Rao, A. M.; Lyuksyutov, S.; Itkis, M. E.; Hamon, M. A.; Hu, H.; Cohn, R. W.; Eklund, P. C.; Colbert, D. T.; Smalley, R. E.; Haddon, R. C. *J. Phys. Chem. B* **2001**, *105*, 2525–2528.
- (14) O'Connell, M. C.; Boul, P.; Ericson, L. M.; Huffman, C.; Wang, Y.; Haroz, E.; Kuper, C.; Tour, J.; Ausman, K. D.; Smalley, R. E. *Chem. Phys. Lett.* **2001**, *342*, 265–271.
- (15) Chattopadhyay, D.; Lastella, S.; Kim, S.; Papadimitrakopoulos, F. *J. Am. Chem. Soc.* **2002**, *124*, 728–729.
- (16) Chattopadhyay, D.; Galeska, I.; Papadimitrakopoulos, F. *J. Am. Chem. Soc.* **2003**, *125*, 3370–3375.
- (17) Hamon, M. A.; Hu, H.; Bhowmik, P.; Niyogi, S.; Zhao, B.; Itkis, M. E.; Haddon, R. C. *Chem. Phys. Lett.* **2001**, *347*, 8–12.
- (18) Bahr, J. L.; Tour, J. M. *Chem. Mater.* **2001**, *13*, 3823–3824.
- (19) Joiasse, C. A. P.; Grablowitz, H.; Pennings, A. J. *Macromol. Chem. Phys.* **2000**, *201*, 107–122.
- (20) Turunen, M. P. K.; Korhonen, H.; Tuominen, J.; Seppälä, J. *V. Polym. Int.* **2001**, *51*, 92–100.
- (21) Lang, M.; Wong, R. P.; Chu, C. C. *J. Polym. Sci., Part A: Polym. Chem.* **2002**, *40*, 1127–1141.
- (22) Maglio, G.; Nese, G.; Nuzzo, M.; Palumbo, R. *Macromol. Rapid Commun.* **2004**, *25*, 1139–1144.
- (23) Lepoitevin, B.; Pantoustier, N.; Alexandre, M.; Calberg, C.; Jérôme, R.; Dubois, P. *J. Mater. Chem.* **2002**, *12*, 3528–3532.
- (24) Qin, S.; Qin, D.; Ford, W. T.; Resasco, D. E.; Herrera, J. E. *J. Am. Chem. Soc.* **2004**, *126*, 170–176.
- (25) Qin, S.; Qin, D.; Ford, W. T.; Resasco, D. E.; Herrera, J. E. *Macromolecules* **2004**, *37*, 752–757.
- (26) Xu, Y.; Gao, C.; Kong, H.; Yan, D.; Jin, Y. Z.; Watts, P. C. P. *Macromolecules* **2004**, *37*, 8846–8853.
- (27) Uhrich, K. E.; et al. *Chem. Rev.* **1999**, *99*, 3181.
- (28) Dobrzynski, P.; Kasperczyk, J.; Bero, M. *Macromolecules* **1999**, *32*, 4735.
- (29) Resasco, D. E.; Alvarez, W. E.; Pompeo, F.; Balzano, L.; Herrera, J. E.; Kitiyanan, B.; Borgna, A. *J. Nanoparticle Res.* **2002**, *4*, 131–136.
- (30) Alvarez, W. E.; Pompeo, F.; Herrera, J. E.; Balzano, L.; Resasco, D. E. *Chem. Mater.* **2002**, *14*, 1853.
- (31) Herrera, J. E.; Balzano, L.; Pompeo, F.; Resasco, D. E. *J. Nanosci. Nanotechnol.* **2003**, *3*, 133.
- (32) Bachilo, S. M.; Balzano, L.; Herrera, J. E.; Pompeo, F.; Resasco, D. E.; Weisman, R. B. *J. Am. Chem. Soc.* **2003**, *125*, 11186–11187.
- (33) Bahr, J. L.; Yang, J.; Kosynkin, D. V.; Bronikowski, M. J.; Smalley, R. E.; Tour, J. M. *J. Am. Chem. Soc.* **2001**, *123*, 6536–6542.
- (34) Weisman, R. B.; Bachilo, S. M. *Nano Lett.* **2003**, *3*, 1235–1238.
- (35) Wunderlich, B.; Cheng, S. Z. D.; Loufakis, K. In *Encyclopedia of Polymer Science and Engineering*, 2nd ed.; Mark, H. F., Bikales, N. M., Overberger, C. G., Menges, G., Kroschwitz, J. I., Eds.; Wiley-Interscience: New York, 1985; Vol. 16, p 777.

MA050876W